

GameFormer: Game-theoretic Modeling and Learning of Transformer-based Interactive Prediction and Planning for Autonomous Driving

Zhiyu Huang[†], Haochen Liu[†], Chen Lv^{*}

Nanyang Technological University, Singapore

[†] Equal contribution {zhiyu001, haochen002}@e.ntu.edu.sg

^{*} Corresponding author lyuchen@ntu.edu.sg

Abstract

Autonomous vehicles operating in complex real-world environments require accurate predictions of interactive behaviors between traffic participants. While existing works focus on modeling agent interactions based on their past trajectories, their future interactions are often ignored. This paper addresses the interaction prediction problem by formulating it with hierarchical game theory and proposing the GameFormer framework to implement it. Specifically, we present a novel Transformer decoder structure that uses the prediction results from the previous level together with the common environment background to iteratively refine the interaction process. Moreover, we propose a learning process that regulates an agent’s behavior at the current level to respond to other agents’ behaviors from the last level. Through experiments on a large-scale real-world driving dataset, we demonstrate that our model can achieve state-of-the-art prediction accuracy on the interaction prediction task. We also validate the model’s capability to jointly reason about the ego agent’s motion plans and other agents’ behaviors in both open-loop and closed-loop planning tests, outperforming a variety of baseline methods. Project website: <https://mczhi.github.io/GameFormer/>

1. Introduction

Accurately forecasting the future behaviors of surrounding traffic participants and making safe and socially-compatible decisions are critical capabilities for modern autonomous driving systems. However, predicting a traffic participant’s future behavior is a highly challenging task due to the heavy reliance of their behaviors on road structures, traffic norms, and underlying interactions among road users. In recent years, deep neural network-based approaches have enjoyed tremendous growth and exhibited significant improvements in prediction accuracy and scalability [7, 11, 14, 36]. In particular, Transformer modules have gained widespread popularity in motion prediction models [22, 28, 29, 32, 41, 43] because of their flexibility and

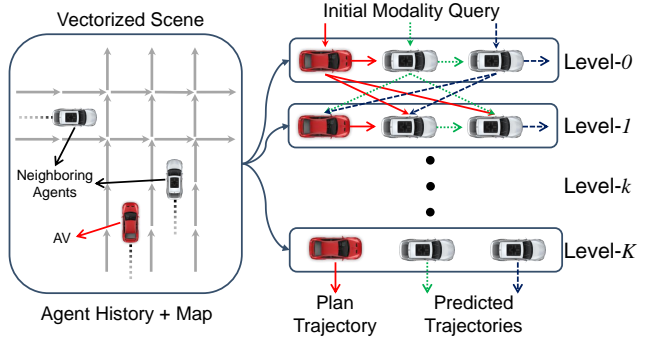


Figure 1. Hierarchical game theoretic modeling of agent interactions. The historical states of agents and maps are encoded as background information; a level-0 agent’s future trajectories are decoded independently based on the initial modality query; a level- k agent responds to all other level- $(k-1)$ agents.

effectiveness in processing information about the driving scene with a heterogeneous mix of modalities (e.g., road maps, traffic signals, and historical states of agents), as well as their ability to capture relationships among these heterogeneous elements.

However, the majority of existing prediction models primarily focus on encoding the driving scene and representing the interaction through the agents’ past trajectories, without explicitly modeling the agents’ future interactions. In addition, most existing models have a significant drawback in that they ignore the interaction with the autonomous vehicle (AV). Consequently, the AV’s downstream planning module has to react to the prediction results passively. However, in critical situations such as merges, lane changes, and unprotected turns, the AV needs to move actively to seek coordination with other agents. Joint prediction and planning is required to deliver more human-like and socially compatible decisions. One typical approach to address this issue is the recently-proposed conditional prediction model [8, 17, 31, 33–35]. This model uses the AV’s internal plans to forecast other agents’ responses to the AV. Although the conditional prediction model mitigates the interaction issue, such a one-way interaction scheme still neglects the dynamic mutual influences between the AV and other road

users. From a game theory perspective, the current prediction/planning models can be regarded as *leader-follower games* with limited interaction levels among agents.

In this study, we utilize a hierarchical game-theoretic framework [15, 25, 37] to model the mutual interactions among agents and propose a new Transformer-based model named *GameFormer* for interactive prediction and planning. As illustrated in Fig. 1, we employ *hierarchical reasoning games* to model the future interactions among agents in an iterative manner to better reflect the cognitive reasoning process. First, we encode the driving scene as background information, which includes vectorized maps and observed agent states, using Transformer encoders. In the future decoding stage, we follow the level- k game theory [5, 38], which assumes that an agent performs a limited number of iterations of strategic reasoning. A level-0 agent acts independently without considering other agents, whereas a level- k agent reacts to the belief that all other agents are level- $(k-1)$. Concretely, we set up a series of Transformer decoders to implement level- k reasoning. The level-0 decoder uses only the initial modality query and encoded scene context as key and value to predict the agent’s multi-modal future trajectories. Then, at each iteration k , the level- k decoder takes as input the predicted trajectories from the level- $(k-1)$ decoder, along with the background information, to predict the agent’s trajectories at the current level. Moreover, we design a learning process that regulates the agents’ trajectories to avoid collision with the trajectories of other agents from the last level while also staying close to human driving data. We train the proposed framework on a large-scale real-world driving dataset and set up two model variants to evaluate our approach’s prediction performance and planning performance in both open-loop and closed-loop settings. The main contributions of this paper are summarized as follows:

1. We propose *GameFormer*, a Transformer-based interactive prediction and planning framework that utilizes hierarchical reasoning to model agent interactions.
2. We design a learning process to train the framework based on the level- k game formalism.
3. We demonstrate the state-of-the-art prediction performance of our model on the Waymo interaction prediction benchmark.
4. We validate the framework’s planning performance in open-loop driving scenes and closed-loop simulations and investigate the effects of game theory settings.

2. Related Work

2.1. Motion Prediction for Autonomous Driving

A rapidly growing line of research on motion prediction studies a new paradigm of forecasting traffic participants’ future trajectories with deep neural networks. These mod-

els have shown powerful capabilities in encoding the scene context, which typically involves road maps and agent history states, resulting in improved prediction accuracy. Early works in this area utilized long short term memory (LSTM) networks [1] to encode the agent’s past states and convolutional neural networks (CNNs) to process the rasterized image of the scene [7, 12, 21, 31]. To explicitly model the interaction between agents, graph neural networks (GNNs) [4, 13, 20, 27] have been widely used to process the scene graph and capture the relationship between agents. More recently, the unified Transformer encoder-decoder structure for motion prediction has gained traction due to its compact model description and superior performance, exemplified by models such as SceneTransformer [29] and WayFormer [28]. However, most Transformer-based prediction models tend to focus more on the encoding part, with less attention paid to the decoding part. Motion Transformer [32] addresses this limitation by proposing a well-designed decoding stage that leverages iterative local motion refinement to enhance prediction accuracy. Inspired by the idea of iterative refinement and hierarchical game theory, we propose a novel Transformer-based decoder for interaction prediction, providing an explicit way to model the interactions between agents. Another issue with existing motion prediction models is they often ignore the active influence of the AV, making them unsuitable for downstream planning tasks. To tackle this problem, various conditional motion prediction models [8, 17, 33] are proposed by informing the prediction process with the planning of the AV. However, these models are still one-way interactions, disregarding the mutual influence between the AV and other agents. In contrast, our approach aims to jointly predict the future trajectories of surrounding agents and plan for the AV through iterative mutual interaction modeling.

2.2. Learning for Decision-making

The primary goal of the motion prediction module is to enable the planning module to make safe and intelligent decisions. This can be achieved through the use of offline learning methods that can learn decision-making from large-scale driving datasets. Imitation learning is the most widely used approach, which aims to learn a driving policy that can replicate expert demonstrations [2, 19, 40]. Offline reinforcement learning [24] has also gained interest as it combines the benefits of reinforcement learning and large collected datasets. However, directly learning a policy lacks interpretability and safety guarantees, and often suffers from distributional shifts. In contrast, planning with a learned motion prediction model is believed to be more interpretable and robust [3, 6, 18, 42], making it a more desirable way for autonomous driving. Our proposed approach aims to enhance the capability of prediction models that can improve interactive decision-making performance.

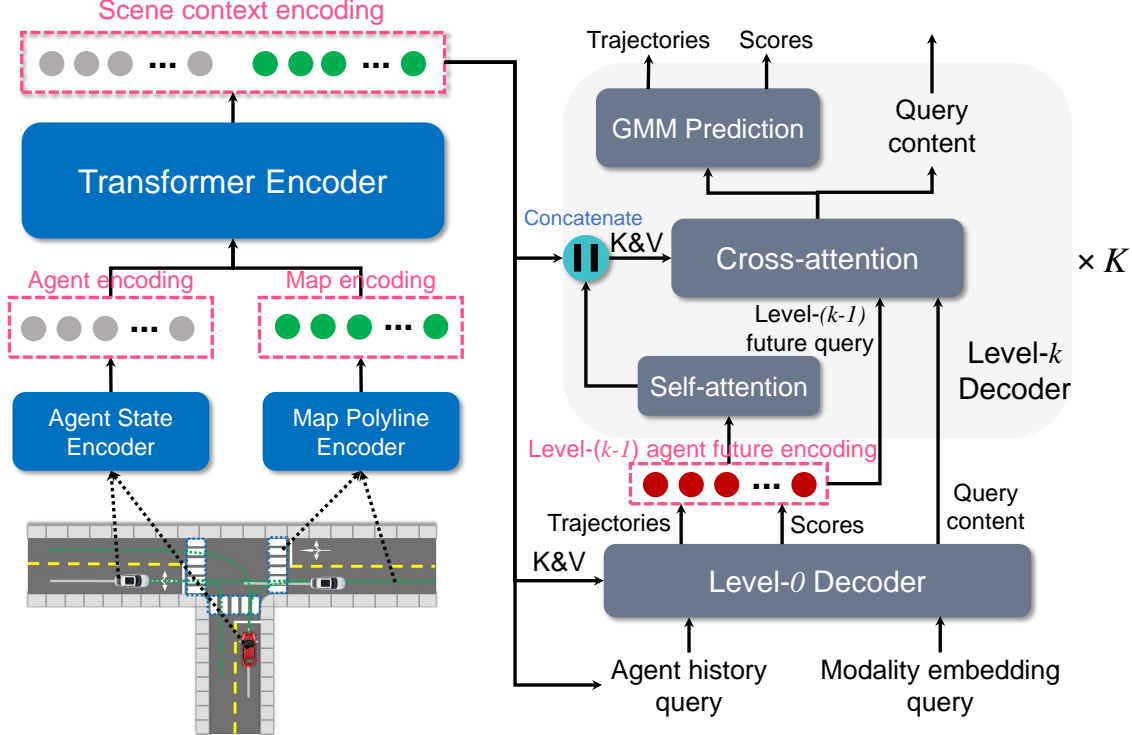


Figure 2. Overview of our proposed *GameFormer* framework. The scene context encoding is obtained via a Transformer-based encoder; the level-0 decoder takes the modality embedding and agent history encodings as query and outputs level-0 future trajectories and scores; the level- k decoder uses a self-attention module to model the level- $(k-1)$ future interaction and append it to the scene context encoding.

3. GameFormer

We introduce our interactive motion prediction and planning framework, called *GameFormer*, which adopts the Transformer encoder-decoder architecture (see Fig. 2). In the following sections, we first define the problem and discuss the level- k game theory that guides the design of the model and learning process in Sec. 3.1. We then describe the encoder component of the model, which encodes the scene context, in Sec. 3.2, and the decoder component, which incorporates a novel interaction modeling concept, in Sec. 3.3. Finally, we present the learning process that accounts for interactions among different reasoning levels in Sec. 3.4.

3.1. Game-theoretic Formulation

We consider a driving scene with N agents, where the AV is denoted as A_0 and its neighboring agents as A_1, \dots, A_{N-1} at the current time $t = 0$. Given the historical states of all agents (including the AV) over an observation horizon T_h , $\mathbf{S} = \{\mathbf{s}_i^{-T_h:0}\}$, as well as the map information \mathbf{M} including traffic lights and road waypoints, the goal is to jointly predict the future trajectories of neighboring agents $\mathbf{Y}_{1:N-1}^{1:T_f}$ over the future horizon T_f , as well as a planned trajectory for the AV $\mathbf{Y}_0^{1:T_f}$. In order to capture the uncertainty, the results are multi-modal future tra-

jectories for the AV and neighboring agents, denoted by $\mathbf{Y}_i^{1:T_f} = \{\mathbf{y}_j^{1:T_f}, p_j | j = 1 : M\}$, where $\mathbf{y}_j^{1:T_f}$ is a sequence of predicted states, p_j the probability of the trajectory, and M the number of modalities.

We leverage level- k game theory to model agent interactions in an iterative manner. Instead of simply predicting a single set of trajectories, we predict a hierarchy of trajectories to model the cognitive interaction process. At each reasoning level, with the exception of level-0, the decoder takes as input the prediction results from the previous level, which effectively makes them a part of the scene, and estimates the responses of agents in the current level to other agents in the previous level. We denote the predicted multi-modal trajectories (essentially a Gaussian mixture model) of agent i at reasoning level k as $\pi_i^{(k)}$, which can be regarded as a policy for that agent. The policy $\pi_i^{(k)}$ is conditioned on the policies of all other agents except the i -th agent at level- $(k-1)$, denoted by $\pi_{-i}^{(k-1)}$. For instance, the AV's policy at level-2 $\pi_0^{(2)}$ would take into account all neighboring agents' policies at level-1 $\pi_{1:N-1}^{(1)}$. Formally, the i -th agent's level- k policy is set to optimize the following objective:

$$\min_{\pi_i} \mathcal{L}_i^k \left(\pi_i^{(k)} | \pi_{-i}^{(k-1)} \right), \quad (1)$$

where $\mathcal{L}(\cdot)$ is the loss (or cost) function. It is important to note that policy π here represents the multi-modal predicted

trajectories (GMM) of an agent and that the loss function is calculated on the trajectory level.

For the level-0 policies, they do not take into account probable actions or reactions of other agents and instead behave independently. Based on the level- k game theory framework, we design the future decoder, which we elaborate upon in Section 3.3.

3.2. Scene Encoding

Input representation. The input data comprises historical state information of agents, $S_p \in \mathbb{R}^{N \times T_h \times d_s}$, where d_s represents the number of state attributes, and local vectorized map polylines $M \in \mathbb{R}^{N \times N_m \times N_p \times d_p}$. For each agent, we find N_m nearby map elements such as routes and cross-walks, each containing N_p waypoints with d_p attributes. The inputs are normalized according to the state of the ego agent, and any missing positions in the tensors are padded with zeros.

Agent History Encoding. We use LSTM networks to encode the historical state sequence S_p for each agent, resulting in a tensor $A_p \in \mathbb{R}^{N \times D}$, which contains the past features of all agents. Here, D denotes the hidden feature dimension.

Vectorized Map Encoding. To encode the local map polylines of all agents, we use the multi-layer perceptron (MLP) network, which generates a map feature tensor $M_p \in \mathbb{R}^{N \times N_m \times N_p \times D}$ with a feature dimension of D . We then group the waypoints from the same map element and use max-pooling to aggregate their features, reducing the number of map tokens. The resulting map feature tensor is reshaped into $M_r \in \mathbb{R}^{N \times N_{mr} \times D}$, where N_{mr} represents the number of aggregated map elements.

Relation Encoding. We concatenate the agent features and their corresponding local map features to create an agent-wise scene context tensor $C^i = [A_p, M_p^i] \in \mathbb{R}^{(N+N_{mr}) \times D}$ for each agent. We use a Transformer encoder with E layers to capture the relationships among all the scene elements in each agent’s context tensor C^i . The Transformer encoder is applied to all agents, generating a final scene context encoding $C_s \in \mathbb{R}^{N \times (N+N_{mr}) \times D}$, which represents the common environment background inputs for the subsequent decoder network.

3.3. Future Decoding with Level- k Reasoning

Modality embedding. To account for future uncertainties, we need to initialize the modality embedding for each possible future, which serves as the query to the level-0 decoder. This can be achieved through either a heuristics-based method, learnable initial queries [28], or through a data-driven method [32]. Specifically, a learnable initial modality embedding tensor $I \in \mathbb{R}^{N \times M \times D}$ is generated, where M represents the number of future modalities.

Level-0 Decoding. In the level-0 decoding layer, a multi-head cross-attention Transformer module is utilized, which takes as input the combination of the initial modality embedding I and the agent’s historical encoding in the final scene context C_{s, A_p} (by inflating a modality axis), resulting in $(C_{s, A_p} + I) \in \mathbb{R}^{N \times M \times D}$ as the query and the scene context encoding C_s as the key and value. The attention is applied to the modality axis for each agent, and the query content features can be obtained after the attention layer as $Z_{L_0} \in \mathbb{R}^{N \times M \times D}$. Two MLPs are appended to the query content features Z_{L_0} to decode the GMM components of predicted futures $G_{L_0} \in \mathbb{R}^{N \times M \times T_f \times 4}$ (corresponding to $(\mu_x, \mu_y, \log \sigma_x, \log \sigma_y)$ at every timestep) and the scores of these components $P_{L_0} \in \mathbb{R}^{N \times M \times 1}$.

Interaction Decoding. The interaction decoding stage contains K decoding layers corresponding to K reasoning levels. In the level- k layer ($k \geq 1$), it receives all agents’ trajectories from the level- $(k-1)$ layer $S_f^{L_{k-1}} \in \mathbb{R}^{N \times M \times T_f \times 2}$ (the mean values of the GMM $G_{L_{k-1}}$) and use an MLP with max-pooling on the time axis to encode the trajectories, resulting in a tensor of agent multi-modal future trajectory encoding $A_{mf}^{L_{k-1}} \in \mathbb{R}^{N \times M \times D}$. Then, we apply weighted-average-pooling on the modality axis with the predicted scores from the level- $(k-1)$ layer $P_{L_{k-1}}$ to obtain the agent future features $A_f^{L_{k-1}} \in \mathbb{R}^{N \times D}$. We use a multi-head self-attention Transformer module to model the interactions between agent future trajectories $A_{fi}^{L_{k-1}}$ and concatenate the resulting interaction features with the scene context encoding from the encoder part. This yields an updated scene context encoding for agent i , denoted by $C_{L_k}^i = [A_{fi}^{L_{k-1}}, C_s^i] \in \mathbb{R}^{(N+N_m+N) \times D}$. We adopt a multi-head cross-attention Transformer module with the query content features from the level- $(k-1)$ layer $Z_{L_{k-1}}^i$ and agent future features $A_{mf}^{L_{k-1}}, (Z_{L_{k-1}}^i + A_{mf}^{i, L_{k-1}}) \in \mathbb{R}^{M \times D}$ as query and the updated scene context encoding $C_{L_k}^i$ as key and value. We use a masking strategy to prevent an agent from accessing its own future information from the last layer. For example, agent A_0 can only get access to the future interaction features of other agents $\{A_1, \dots, A_{N-1}\}$. Finally, the resulting query content tensor from the cross-attention module $Z_{L_k}^i$ is passed through two MLPs to decode the agent’s GMM components and scores, respectively. Fig. 3 illustrates the detailed structure of a level- k interaction decoder. Note that we share the level- k decoder for all agents to generate multi-agent trajectories at that level. At the final level of interaction decoding, we can obtain multi-modal trajectories for the AV and neighboring agents G_{L_K} , as well as their scores P_{L_K} .

3.4. Learning Process

We propose a learning process to train our model using the level- k game theory formalism. For a level- k agent

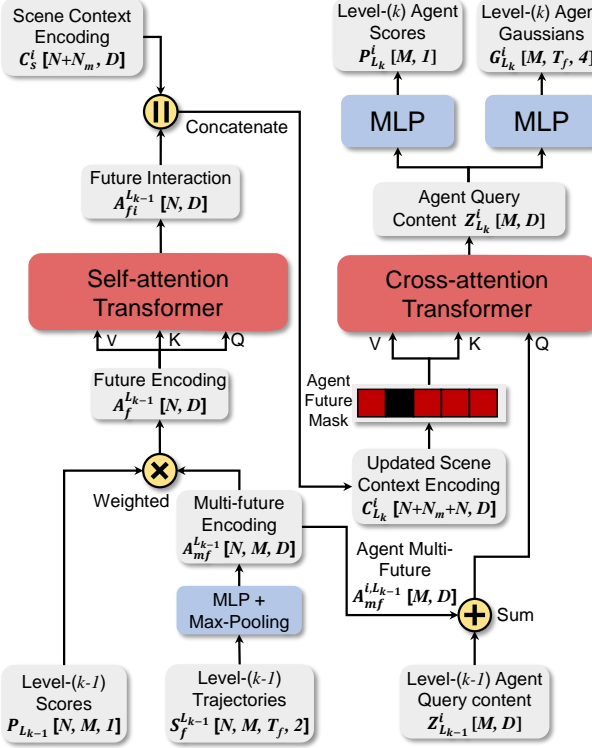


Figure 3. The detailed structure of a level- k interaction decoder.

$A_i^{(k)}$, we design a loss function inspired by prior works [4, 16, 26] that considers the agent’s interactions with others. The safety of agent interactions is crucial, and we use an interaction loss (applicable only to decoding levels $k \geq 1$) to encourage the agent to avoid collisions with the possible future trajectories of other level- $(k-1)$ agents. Specifically, we use a repulsive potential field in the interaction loss to discourage the agent’s future trajectories from getting too close to any possible trajectory of any other level- $(k-1)$ agent $A_{\neg i}^{(k-1)}$. The interaction loss is defined as follows:

$$\mathcal{L}_{Inter} = \sum_{m=1}^M \sum_{t=1}^{T_f} \max_{\forall j \neq i \atop \forall n \in 1:M} \frac{1}{d(\hat{s}_{m,t}^{(i,k)}, \hat{s}_{n,t}^{(j,k-1)}) + 1}, \quad (2)$$

where $d(\cdot, \cdot)$ is the L_2 distance between the future states $((x, y)$ positions), m is the mode of the agent i , n is the mode of the level- $(k-1)$ agent j , and we introduce a safety margin to ensure that the repulsive force is only active when the distance is close enough.

We also include imitation loss to regularize the agent’s behaviors, which can be seen as a surrogate for other factors such as traffic rules and driving styles. The future behavior of an agent is modeled as a Gaussian mixture model (GMM), where each mode m at each time step t is represented by a Gaussian distribution over (x, y) , characterized by a mean μ_m^t and covariance σ_m^t . We use the negative log-likelihood loss at each timestep in the best-predicted com-

ponent m^* (closest to the ground truth) to calculate the imitation loss.

$$\mathcal{L}_{IL} = \sum_{t=1}^{T_f} \mathcal{L}_{NLL}(\mu_{m^*}^t, \sigma_{m^*}^t, p_{m^*}, \mathbf{s}_t), \quad (3)$$

where \mathcal{L}_{NLL} is the negative log-likelihood loss function given by:

$$\mathcal{L}_{NLL} = \log \sigma_x + \log \sigma_y + \frac{1}{2} \left(\left(\frac{dx}{\sigma_x} \right)^2 + \left(\frac{dy}{\sigma_y} \right)^2 \right) - \log(p_{m^*}), \quad (4)$$

where $d_x = \mathbf{s}_x - \mu_x$ and $d_y = \mathbf{s}_y - \mu_y$, $(\mathbf{s}_x, \mathbf{s}_y)$ is ground-truth position; p_{m^*} is the probability of the selected component, and we use the cross-entropy loss in practice.

The total loss function for the level- k agent i is the weighted sum of the interaction loss and imitation loss.

$$\mathcal{L}_i^k(\pi_i^{(k)}) = w_1 \mathcal{L}_{IL}(\pi_i^{(k)}) + w_2 \mathcal{L}_{Inter}(\pi_i^{(k)}, \pi_{\neg i}^{(k-1)}), \quad (5)$$

where w_1 and w_2 are the weighting factors to balance the influence of the two loss terms.

4. Experiments

4.1. Experimental Setup

Dataset. Our approach is trained and evaluated on the large-scale driving dataset, Waymo open motion dataset (WOMD) [9], which contains abundant and diverse human interactions from real-world traffic scenes. We set up two different model variants for different evaluation purposes.

Prediction-oriented model. This model variant focuses on improving prediction accuracy, especially in interaction prediction. We adopt the setting of the WOMD interaction prediction task, where the model predicts the joint future positions of two interacting agents 8 seconds into the future, based on their one second of historical data and high-definition maps. The neighboring agents within the scene will serve as the background information in the encoding stage, while only the two labeled interacting agents’ joint future trajectories are predicted. The model is trained on the entire WOMD training dataset, and we adhere to the official evaluation metrics, which include minimum average displacement error (minADE), minimum final displacement error (minFDE), miss rate, and mean average precision (mAP). We investigate two different interaction prediction settings. Firstly, we consider the joint prediction setting, where only 6 joint trajectories of the two agents are predicted [29]. Secondly, we examine the marginal prediction setting and train our model to predict 64 marginal trajectories for each agent in the interaction pair. During inference, the EM method proposed in MultiPath++ [36] is employed to generate a set of 6 marginal trajectories for each agent, from which the top 6 joint predictions are selected for these two agents.

Planning-oriented model. We introduce another model variant that is designed for planning. Specifically, the observation horizon is 1 second and the prediction/planning horizon is set to 5 seconds, and all the neighboring agents' future interactions are considered to predict their future trajectories. We randomly select 10,000 20-second scenarios from the WOMD dataset, where 9,000 scenarios are used for training and the remaining 1,000 for validation. Furthermore, we evaluate the model's joint prediction and planning performance on 400 9-second scenarios¹, which includes interesting interactions such as lane-change, merge, and left-turn. To conduct closed-loop testing, we utilize a log-replay simulator to replay the original scenarios and override the AV with our planner. In addition, to improve the closed-loop planning performance, we employ a motion planner [18] to refine the trajectory provided by the model by explicitly optimizing the trajectory's cost. In open-loop testing, we use distance-based error metrics, including planning ADE, collision rate, miss rate, and prediction ADE. In closed-loop testing, we focus on evaluating the planner's performance in a realistic driving scenario by measuring metrics including collision rate, off-route rate, progress along the route, longitudinal acceleration and jerk, lateral acceleration, and position errors. More information about our models is provided in the supplementary material.

Implementation Details. To encode the scene context, we use a stack of $E = 6$ Transformer encoder layers, and the hidden feature dimension is set to $D = 256$. For the prediction-oriented model, we consider 20 neighboring agents around the interacting agents and employ $K = 6$ decoding layers. For the planning-oriented model, we need to balance the trade-off between computation efficiency and prediction accuracy. Thus, we consider 10 neighboring agents closest to the ego agent to predict $M = 6$ joint future trajectories and determine the optimal number of reasoning levels K through experiments. Furthermore, for each agent, its local map elements consist of possible driving lane polylines and crosswalk polylines. More details about the input data and training settings for both models can be found in the supplementary material.

4.2. Main Results

4.2.1 Interaction Prediction

Quantitative results. Table 1 summarizes the prediction performance of our model in comparison with state-of-the-art methods on the WOMD interaction prediction (joint prediction of two interacting agents) benchmark. The metrics are averaged over different object types (vehicle, pedestrian, and cyclist) and evaluation times (3, 5, and 8 seconds). Our $M = 6$ joint prediction model outperforms existing state-of-the-art methods in terms of position errors. This can be

attributed to its superior ability to capture future interactions between agents through an iterative process and to predict future trajectories in a scene-consistent manner. However, the scoring performance of the joint model is limited without predicting an over-complete set of trajectories and aggregation. To mitigate this issue, we employ the $M = 64$ marginal prediction model with EM aggregation, which significantly improves the scoring performance (better mAP metric). The overall performance of our marginal model is comparable to that of the heavily ensembled and much more complex MTR model [32]. Nevertheless, it is worth noting that marginal ensemble models may not be practical for real-world applications due to their substantial computational burden. Therefore, we utilize our joint prediction model, which provides better prediction accuracy and computational efficiency, for planning tests.

Table 1. Comparison with state-of-the-art models on the WOMD interaction prediction benchmark

Model	minADE (↓)	minFDE (↓)	Miss rate (↓)	mAP (↑)
LSTM baseline [9]	1.9056	5.0278	0.7750	0.0524
Heat [27]	1.4197	3.2595	0.7224	0.0844
AIR ² [39]	1.3165	2.7138	0.6230	0.0963
SceneTrans [29]	0.9774	2.1892	0.4942	0.1192
DenseTNT [14]	1.1417	2.4904	0.5350	0.1647
M2I [34]	1.3506	2.8325	0.5538	0.1239
MTR [32]	0.9181	2.0633	0.4411	0.2037
GameFormer (M, $M=64$)	0.9721	2.2146	0.4933	0.1923
GameFormer (J, $M=6$)	0.9161	1.9373	0.4531	0.1376

Qualitative results. Fig. 4 illustrates the interaction prediction performance of our approach in several typical scenarios. In the vehicle-vehicle interaction scenario, two distinct situations are captured by our model: vehicle 2 accelerates to pass the intersection first and vehicle 2 yields to vehicle 1. In both situations, our model predicts that vehicle 1 creeps forward to observe the actions of vehicle 2 before completing a left turn. In the vehicle-pedestrian scenario, our model predicts that the vehicle will stop and wait for the pedestrian to pass before resuming movement. In the vehicle-cyclist interaction scenario, where the vehicle intends to merge into the right lane, our model predicts the vehicle will decelerate and follow behind the cyclist in that lane. Overall, the results manifest that our model can accurately predict the possible joint futures of interacting agents.

4.2.2 Open-loop Planning

Determining the decoding levels. To determine the optimal reasoning levels for planning, we analyze the impact of decoding layers on open-loop planning performance, and the results are presented in Table 2. It can be inferred that the performance reaches its peak when the number of interaction decoding layers is increased to 4. Although the planning ADE and prediction ADE exhibit a slight decrease with additional decoding layers, the miss rate and collision

¹<https://tinyurl.com/3pxvf7cu>

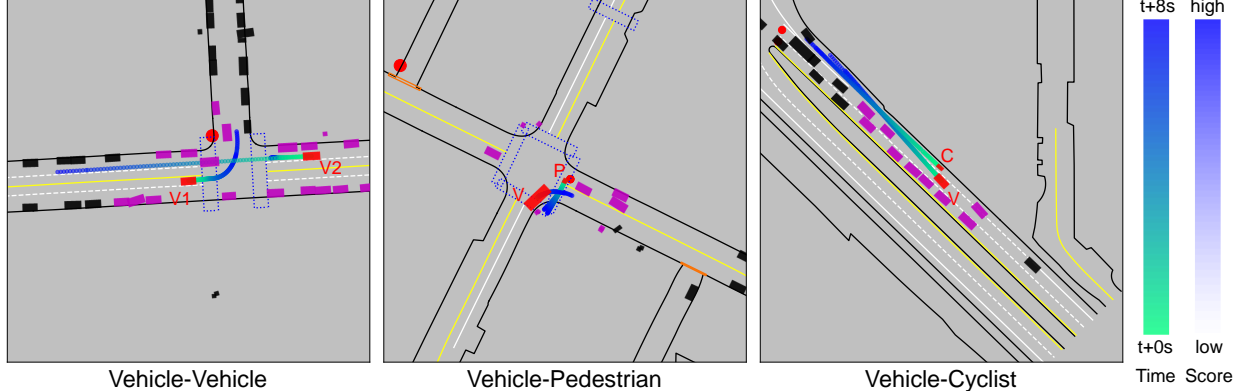


Figure 4. Qualitative results of the proposed method in interaction prediction (multi-modal joint prediction of two interacting agents). The red boxes are interacting agents to predict and the magenta boxes are background neighboring agents.

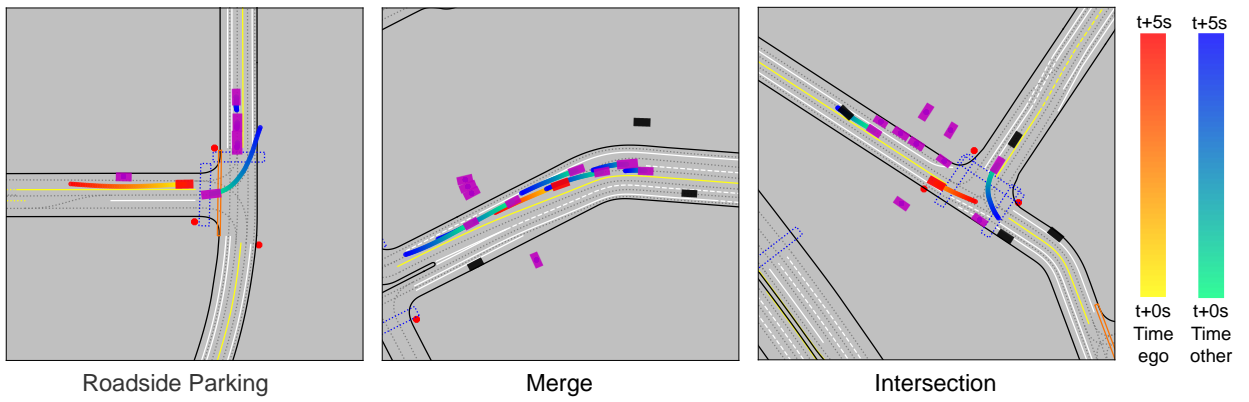


Figure 5. Qualitative results of the proposed method in open-loop planning. The red box is the AV and the magenta boxes are its neighboring agents; the red trajectory is the plan of the AV and the blue ones are the predictions of neighboring agents.

rate are at their lowest when the decoding level is 4. The intuition behind this observation is that humans are capable of performing only a limited depth of reasoning. In our open-loop planning experiments, the optimal iteration depth empirically appears to be 4.

Table 2. Influence of decoding levels on open-loop planning

Level	Planning ADE	Collision Rate	Miss Rate	Prediction ADE
0	0.9458	0.0384	0.1154	1.0955
1	0.8846	0.0305	0.0994	0.9377
2	0.8529	0.0277	0.0897	0.8875
3	0.8423	0.0269	0.0816	0.8723
4	0.8329	0.0198	0.0753	0.8527
5	0.8171	0.0245	0.0777	0.8361
6	0.8208	0.0238	0.0826	0.8355

Quantitative results. Our joint prediction and planning model employs 4 decoding layers, and the results of the final decoding layer (the most-likely future evaluated by the trained scorer) are utilized as the plan for the AV and predictions for other agents. We set up some imitation learning-based planning methods as baselines, which are: 1) vanilla imitation learning (IL), 2) deep imitative model (DIM) [30], 3) MultiPath++ [23,36] (which predicts multi-modal trajectories for the ego agent), 4) MTR-e2e (end-to-end variant

with learnable motion queries) [32], and 5) differentiable integrated prediction and planning (DIPP) [18]. Table 3 reports the open-loop planning performance of our model in comparison with the baseline methods. The results reveal that our model performs significantly better than vanilla IL and DIM, because they are just trained to output the ego’s trajectory while not explicitly predicting other agents’ future behaviors. Compared to performant motion prediction models (MultiPath++ and MTR-e2e), our model also shows better planning metrics for the ego agent. Moreover, our model outperforms DIPP (a joint prediction and planning method) in both planning and prediction metrics, especially the collision rate. These results emphasize the advantage of our model, which explicitly considers all agents’ future behaviors and iteratively refines the interaction process.

Qualitative results. Fig. 5 displays qualitative results of our model’s open-loop planning performance in complex driving scenarios. For clarity, only the most-likely trajectories of the agents are displayed. These results demonstrate that our model can generate a plausible future trajectory for the AV and handle diverse interaction scenarios, and predictions of the surrounding agents enhance the interpretability of our planning model’s output.

Table 3. Evaluation of open-loop planning performance of the proposed method against baseline methods

Method	Collision rate (%)	Miss rate (%)	Planning error (m)			Prediction error (m)	
			@1s	@3s	@5s	ADE	FDE
Vanilla IL	4.25	15.61	0.216	1.273	3.175	–	–
DIM	4.96	17.68	0.483	1.869	3.683	–	–
MultiPath++	2.86	8.61	0.146	0.948	2.719	–	–
MTR-e2e	2.32	8.88	0.141	0.888	2.698	–	–
DIPP	2.33	8.44	0.135	0.928	2.803	0.925	2.059
Ours	1.98	7.53	0.129	0.836	2.451	0.853	1.919

Table 4. Evaluation of closed-loop planning performance of the proposed method against baseline methods

Method	Collision (%)	Off route (%)	Progress (m)	Acc. (m/s^2)	Jerk (m/s^3)	Lat. acc. (m/s^2)	Position error (m)		
							@3s	@5s	@8s
Vanilla IL	43	57	6.23	1.588	16.24	0.661	9.355	20.52	46.33
RIP	42.5	38	12.85	1.445	14.97	0.355	7.035	17.13	38.25
CQL	49	41	8.28	3.158	25.31	0.152	10.86	21.18	40.17
DIPP (w/ refinement)	7	0	51.80	0.484	1.528	0.071	2.297	5.554	12.10
Ours (w/ refinement)	5.5	0	49.11	0.544	1.927	0.097	2.021	4.871	10.93

4.2.3 Closed-loop Planning

We evaluate the closed-loop planning performance of our model in a simulated environment that replays the logged trajectories of other agents while updating the ego agent’s state according to the planned trajectory. We also employ a refine motion planner that takes the planned trajectory as initialization and other agents’ prediction results to explicitly regulate the AV not to violate traffic rules or cause a collision. The decision-making task was compared against four baseline methods: 1) vanilla IL, 2) robust imitative planning (RIP) [10], 3) conservative Q-learning (CQL) [24], and 4) DIPP [18]. The quantitative results of closed-loop testing are summarized in Table 4, and the visualization results of our model are provided in the supplementary material. Our results show that the IL and offline RL methods performed poorly in the closed-loop test due to distributional shifts. In contrast, planning-based methods (DIPP and ours) perform significantly better across all metrics, but their performance relies on accurate prediction of other agents and a good initialization of the plan. Our method outperforms DIPP in terms of position error and collision rate because our model can deliver better prediction of the agent interactions and provide a good initial plan to the motion planner. Note that the collision rate is a lower bound on safety since other agents do not react to the ego agent.

4.3. Ablation study

Effects of agent future modeling. We investigate the impact of different agent future modeling settings on the open-loop planning performance. We compare our base model to three ablated models, which are: 1) *No future* (where agent future trajectories from the last level are not

incorporated in decoding the current level), 2) *No self-attention* (where agent future trajectories are incorporated but not processed by a self-attention module), and 3) *No interaction loss* (where the model is trained without the proposed interaction loss). The results presented in Table 5 indicate that our game-theoretic approach can significantly improve the planning and prediction accuracy by utilizing the future trajectories of agents from the last level as the scene context in the current level. Additionally, incorporating a self-attention module to represent future interactions among agents improves the accuracy, while using the proposed interaction loss to train the model significantly reduces the collision rate. Further ablation experiments can be found in the supplementary materials.

Table 5. Influence of agent future modeling on open-loop planning

	Planning ADE	Collision Rate	Miss Rate	Prediction ADE
No future	0.9210	0.0295	0.0963	0.9235
No self-attention	0.8666	0.0231	0.0860	0.8856
No interaction loss	0.8415	0.0417	0.0846	0.8486
Base	0.8329	0.0198	0.0753	0.8527

5. Conclusions

This paper introduces *GameFormer*, a Transformer-based model that utilizes hierarchical game theory for interactive prediction and planning. Our proposed approach incorporates novel level- k decoders in the prediction model that iteratively refine the future trajectories of interacting agents, as well as a learning process that regulates the predicted behaviors of agents given the prediction results from the last level. Experimental results on the Waymo open dataset demonstrate that our model achieves state-of-the-art accuracy in interaction prediction and outperforms baseline methods in both open-loop and closed-loop planning tests.

References

[1] Alexandre Alahi, Kratarth Goel, Vignesh Ramanathan, Alexandre Robicquet, Li Fei-Fei, and Silvio Savarese. Social lstm: Human trajectory prediction in crowded spaces. In *Proceedings of the IEEE conference on computer vision and pattern recognition*, pages 961–971, 2016. [2](#)

[2] Mayank Bansal, Alex Krizhevsky, and Abhijit Ogale. Chauffeurnet: Learning to drive by imitating the best and synthesizing the worst. *arXiv preprint arXiv:1812.03079*, 2018. [2](#)

[3] Sergio Casas, Abbas Sadat, and Raquel Urtasun. Mp3: A unified model to map, perceive, predict and plan. In *Proceedings of the IEEE/CVF Conference on Computer Vision and Pattern Recognition*, pages 14403–14412, 2021. [2](#)

[4] Yuxiao Chen, Boris Ivanovic, and Marco Pavone. Scept: Scene-consistent, policy-based trajectory predictions for planning. In *Proceedings of the IEEE/CVF Conference on Computer Vision and Pattern Recognition*, pages 17103–17112, 2022. [2, 5](#)

[5] Miguel A Costa-Gomes, Vincent P Crawford, and Nagore Iribarri. Comparing models of strategic thinking in van huyck, battalio, and beil’s coordination games. *Journal of the European Economic Association*, 7(2-3):365–376, 2009. [2](#)

[6] Alexander Cui, Sergio Casas, Abbas Sadat, Renjie Liao, and Raquel Urtasun. Lookout: Diverse multi-future prediction and planning for self-driving. In *Proceedings of the IEEE/CVF International Conference on Computer Vision*, pages 16107–16116, 2021. [2](#)

[7] Henggang Cui, Vladan Radosavljevic, Fang-Chieh Chou, Tsung-Han Lin, Thi Nguyen, Tzu-Kuo Huang, Jeff Schneider, and Nemanja Djuric. Multimodal trajectory predictions for autonomous driving using deep convolutional networks. In *2019 International Conference on Robotics and Automation (ICRA)*, pages 2090–2096. IEEE, 2019. [1, 2](#)

[8] Jose Luis Vazquez Espinoza, Alexander Liniger, Wilko Schwarting, Daniela Rus, and Luc Van Gool. Deep interactive motion prediction and planning: Playing games with motion prediction models. In *Learning for Dynamics and Control Conference*, pages 1006–1019. PMLR, 2022. [1, 2](#)

[9] Scott Ettinger, Shuyang Cheng, Benjamin Caine, Chenxi Liu, Hang Zhao, Sabeek Pradhan, Yuning Chai, Ben Sapp, Charles R Qi, Yin Zhou, et al. Large scale interactive motion forecasting for autonomous driving: The waymo open motion dataset. In *Proceedings of the IEEE/CVF International Conference on Computer Vision*, pages 9710–9719, 2021. [5, 6](#)

[10] Angelos Filos, Panagiotis Tsigkas, Rowan McAllister, Nicholas Rhinehart, Sergey Levine, and Yarin Gal. Can autonomous vehicles identify, recover from, and adapt to distribution shifts? In *International Conference on Machine Learning*, pages 3145–3153. PMLR, 2020. [8](#)

[11] Jiyang Gao, Chen Sun, Hang Zhao, Yi Shen, Dragomir Anguelov, Congcong Li, and Cordelia Schmid. Vectornet: Encoding hd maps and agent dynamics from vectorized representation. In *Proceedings of the IEEE/CVF Conference on Computer Vision and Pattern Recognition*, pages 11525–11533, 2020. [1](#)

[12] Thomas Gilles, Stefano Sabatini, Dzmitry Tsishkou, Bogdan Stanciulescu, and Fabien Moutarde. Home: Heatmap output for future motion estimation. In *2021 IEEE International Intelligent Transportation Systems Conference (ITSC)*, pages 500–507. IEEE, 2021. [2](#)

[13] Thomas Gilles, Stefano Sabatini, Dzmitry Tsishkou, Bogdan Stanciulescu, and Fabien Moutarde. Gohome: Graph-oriented heatmap output for future motion estimation. In *2022 International Conference on Robotics and Automation (ICRA)*, pages 9107–9114. IEEE, 2022. [2](#)

[14] Junru Gu, Chen Sun, and Hang Zhao. Densetnt: End-to-end trajectory prediction from dense goal sets. In *Proceedings of the IEEE/CVF International Conference on Computer Vision*, pages 15303–15312, 2021. [1, 6](#)

[15] Peng Hang, Chen Lv, Chao Huang, Yang Xing, and Zhongxu Hu. Cooperative decision making of connected automated vehicles at multi-lane merging zone: A coalitional game approach. *IEEE Transactions on Intelligent Transportation Systems*, 23(4):3829–3841, 2021. [2](#)

[16] Niklas Hanselmann, Katrin Renz, Kashyap Chitta, Apratim Bhattacharyya, and Andreas Geiger. King: Generating safety-critical driving scenarios for robust imitation via kinematics gradients. *arXiv preprint arXiv:2204.13683*, 2022. [5](#)

[17] Zhiyu Huang, Haochen Liu, Jingda Wu, and Chen Lv. Conditional predictive behavior planning with inverse reinforcement learning for human-like autonomous driving. *arXiv preprint arXiv:2212.08787*, 2022. [1, 2](#)

[18] Zhiyu Huang, Haochen Liu, Jingda Wu, and Chen Lv. Differentiable integrated motion prediction and planning with learnable cost function for autonomous driving. *arXiv preprint arXiv:2207.10422*, 2022. [2, 6, 7, 8](#)

[19] Zhiyu Huang, Chen Lv, Yang Xing, and Jingda Wu. Multimodal sensor fusion-based deep neural network for end-to-end autonomous driving with scene understanding. *IEEE Sensors Journal*, 21(10):11781–11790, 2020. [2](#)

[20] Zhiyu Huang, Xiaoyu Mo, and Chen Lv. Multi-modal motion prediction with transformer-based neural network for autonomous driving. In *2022 International Conference on Robotics and Automation (ICRA)*, pages 2605–2611. IEEE, 2022. [2](#)

[21] Zhiyu Huang, Xiaoyu Mo, and Chen Lv. Recoat: A deep learning-based framework for multi-modal motion prediction in autonomous driving application. In *2022 IEEE 25th International Conference on Intelligent Transportation Systems (ITSC)*, pages 988–993. IEEE, 2022. [2](#)

[22] Xiaosong Jia, Penghao Wu, Li Chen, Hongyang Li, Yu Liu, and Junchi Yan. Hdgt: Heterogeneous driving graph transformer for multi-agent trajectory prediction via scene encoding. *arXiv preprint arXiv:2205.09753*, 2022. [1](#)

[23] Stepan Konev. Mpa: Multipath++ based architecture for motion prediction. *arXiv preprint arXiv:2206.10041*, 2022. [7](#)

[24] Aviral Kumar, Aurick Zhou, George Tucker, and Sergey Levine. Conservative q-learning for offline reinforcement learning. *Advances in Neural Information Processing Systems*, 33:1179–1191, 2020. [2, 8](#)

[25] Nan Li, Dave W Oyler, Mengxuan Zhang, Yildiray Yildiz, Ilya Kolmanovsky, and Anouck R Girard. Game theoretic

modeling of driver and vehicle interactions for verification and validation of autonomous vehicle control systems. *IEEE Transactions on control systems technology*, 26(5):1782–1797, 2017. 2

[26] Jerry Liu, Wenyuan Zeng, Raquel Urtasun, and Ersin Yumer. Deep structured reactive planning. In *2021 IEEE International Conference on Robotics and Automation (ICRA)*, pages 4897–4904. IEEE, 2021. 5

[27] Xiaoyu Mo, Zhiyu Huang, Yang Xing, and Chen Lv. Multi-agent trajectory prediction with heterogeneous edge-enhanced graph attention network. *IEEE Transactions on Intelligent Transportation Systems*, 2022. 2, 6

[28] Nigamaa Nayakanti, Rami Al-Rfou, Aurick Zhou, Kratarth Goel, Khaled S Refaat, and Benjamin Sapp. Wayformer: Motion forecasting via simple & efficient attention networks. *arXiv preprint arXiv:2207.05844*, 2022. 1, 2, 4

[29] Jiquan Ngiam, Vijay Vasudevan, Benjamin Caine, Zhengdong Zhang, Hao-Tien Lewis Chiang, Jeffrey Ling, Rebecca Roelofs, Alex Bewley, Chenxi Liu, Ashish Venugopal, et al. Scene transformer: A unified architecture for predicting future trajectories of multiple agents. In *International Conference on Learning Representations*, 2021. 1, 2, 5, 6

[30] Nicholas Rhinehart, Rowan McAllister, and Sergey Levine. Deep imitative models for flexible inference, planning, and control. In *International Conference on Learning Representations*, 2019. 7

[31] Tim Salzmann, Boris Ivanovic, Punarjay Chakravarty, and Marco Pavone. Trajectron++: Dynamically-feasible trajectory forecasting with heterogeneous data. In *European Conference on Computer Vision*, pages 683–700. Springer, 2020. 1, 2

[32] Shaoshuai Shi, Li Jiang, Dengxin Dai, and Bernt Schiele. Motion transformer with global intention localization and local movement refinement. *Advances in Neural Information Processing Systems*, 2022. 1, 2, 4, 6, 7

[33] Haoran Song, Wenchoao Ding, Yuxuan Chen, Shaojie Shen, Michael Yu Wang, and Qifeng Chen. Pip: Planning-informed trajectory prediction for autonomous driving. In *European Conference on Computer Vision*, pages 598–614. Springer, 2020. 1, 2

[34] Qiao Sun, Xin Huang, Junru Gu, Brian C Williams, and Hang Zhao. M2i: From factored marginal trajectory prediction to interactive prediction. In *Proceedings of the IEEE/CVF Conference on Computer Vision and Pattern Recognition*, pages 6543–6552, 2022. 1, 6

[35] Ekaterina Tolstaya, Reza Mahjourian, Carlton Downey, Balakrishnan Vadarajan, Benjamin Sapp, and Dragomir Anguelov. Identifying driver interactions via conditional behavior prediction. In *2021 IEEE International Conference on Robotics and Automation (ICRA)*, pages 3473–3479. IEEE, 2021. 1

[36] Balakrishnan Varadarajan, Ahmed Hefny, Avikalp Srivastava, Khaled S Refaat, Nigamaa Nayakanti, Andre Cornman, Kan Chen, Bertrand Douillard, Chi Pang Lam, Dragomir Anguelov, et al. Multipath++: Efficient information fusion and trajectory aggregation for behavior prediction. In *2022 International Conference on Robotics and Automation (ICRA)*, pages 7814–7821. IEEE, 2022. 1, 5, 7

[37] Wenshuo Wang, Letian Wang, Chengyuan Zhang, Changliu Liu, and Lijun Sun. Social interactions for autonomous driving: A review and perspectives. *arXiv preprint arXiv:2208.07541*, 2022. 2

[38] James R Wright and Kevin Leyton-Brown. Beyond equilibrium: Predicting human behavior in normal-form games. In *Twenty-Fourth AAAI Conference on Artificial Intelligence*, 2010. 2

[39] David Wu and Yunnan Wu. Air² for interaction prediction. *arXiv preprint arXiv:2111.08184*, 2021. 6

[40] Danfei Xu, Yuxiao Chen, Boris Ivanovic, and Marco Pavone. Bits: Bi-level imitation for traffic simulation. *arXiv preprint arXiv:2208.12403*, 2022. 2

[41] Ye Yuan, Xinshuo Weng, Yanglan Ou, and Kris M Kitani. Agentformer: Agent-aware transformers for socio-temporal multi-agent forecasting. In *Proceedings of the IEEE/CVF International Conference on Computer Vision*, pages 9813–9823, 2021. 1

[42] Wenyuan Zeng, Wenjie Luo, Simon Suo, Abbas Sadat, Bin Yang, Sergio Casas, and Raquel Urtasun. End-to-end interpretable neural motion planner. In *Proceedings of the IEEE/CVF Conference on Computer Vision and Pattern Recognition*, pages 8660–8669, 2019. 2

[43] Zikang Zhou, Luyao Ye, Jianping Wang, Kui Wu, and Kejie Lu. Hivt: Hierarchical vector transformer for multi-agent motion prediction. In *Proceedings of the IEEE/CVF Conference on Computer Vision and Pattern Recognition*, pages 8823–8833, 2022. 1

A. Experiment Details

A.1. Prediction-oriented model

Model inputs. In each scene, one of the two interacting agents is designated as the focal agent, with its current state serving as the origin of the coordinate system. We consider 10 surrounding agents closest to a target agent as the background agents, and therefore, there are two target agents to predict and up to 20 different background agents in a scene. The current and historical states of each agent are retrieved for the last one second at a sampling rate of 10Hz, resulting in a tensor with a shape of (22×11) for each agent. The state at each timestep includes the agent’s position (x, y) , heading angle (θ) , velocity (v_x, v_y) , bounding box size (L, W, H) , and one-hot category mask of the agent (totally three types). All historical states for each agent are aggregated into a fixed-shape tensor of $(22 \times 11 \times 11)$, with missing agent states padded as zeros, to form the input tensor of historical agent states.

For each target agent, up to 6 drivable lanes (each extending 100 meters) that the agent may take are identified using depth first search on the road graph, along with 4 nearby crosswalks as the local map context, with each map vector containing 100 waypoints. The features of a waypoint in a drivable lane include the position and heading angles of the centerline, left boundary, and right boundary, speed limit, as well as discrete attributes such as the lane type, traffic light state, and whether it is controlled by a stop sign. The features of a waypoint in the crosswalk polyline only encompass position and heading angle. Therefore, the local map context for a target agent comprises two tensors: drivable lanes with shape $(6 \times 100 \times 15)$ and crosswalks with shape $(4 \times 100 \times 3)$.

Encoder structure. In the encoder part, we utilize two separate LSTMs to encode the historical states of the target and background agents, respectively, resulting in a tensor with shape (22×256) that encompasses all agents’ historical state sequences. The local map context encoder consists of a lane encoder for processing the drivable lanes and a crosswalk encoder for the crosswalk polylines. The lane encoder employs MLPs to encode numeric features and embedding layers to encode discrete features, outputting a tensor of encoded lane vectors with shape $(2 \times 6 \times 100 \times 256)$, while the crosswalk encoder uses an MLP to encode numeric features, resulting in a tensor of crosswalk vectors with shape $(2 \times 4 \times 100 \times 256)$. Subsequently, we utilize a max-pooling layer (with a step size of 10) to aggregate the waypoints from a drivable lane in the encoded lane tensor, yielding a tensor with shape $(2 \times 6 \times 10 \times 256)$ that is reshaped to $(2 \times 60 \times 256)$. Similarly, the encoded crosswalk tensor is processed using a max-pooling layer with a step size of 20 to obtain a tensor with shape $(2 \times 20 \times 256)$. These two tensors are concatenated to produce an encoded

local map context tensor with shape $(2 \times 80 \times 256)$. For each target agent, we concatenate its local map context tensor with the historical state tensor of all agents to obtain a scene context tensor with dimensions of (102×256) , and we use self-attention Transformer encoder layers to extract the relationships among the elements in the scene. It is important to note that invalid positions in the scene context tensor are masked from attention calculations.

Decoder structure. For $M = 6$ Joint prediction model, we employ the learnable latent modality embedding with a shape of $(2 \times 6 \times 256)$. For each agent, the query (6×256) in the level-0 decoder is obtained by summing up the encoding of the target agent’s history and its corresponding latent modality embedding; the value and key are derived from the scene context by the encoder. The level-0 decoder generates the multi-modal future trajectories of the target agent with x and y coordinates using an MLP from the attention output. The scores of each trajectory are decoded by another MLP with a shape of (6×1) . In a level- k decoder, we use a shared future encoder across different layers, which includes an MLP and a max-pooling layer, to encode the future trajectories from the previous level into a tensor with a shape of (6×256) . Next, we employ the trajectory scores to average-pool the encoded trajectories, which results in the encoded future of the agent. The encoded futures of the two target agents are then fed into a self-attention Transformer layer to model their future interaction. Finally, the output of the Transformer layer is appended to the scene context obtained from the encoder.

For $M = 64$ Marginal prediction mode, we use a set of 64 fixed intention points that are encoded with MLPs to create the modality embedding with shape $(2 \times 64 \times 256)$. This modality embedding serves as the query input for the level-0 decoder. The fixed intention points are obtained through the K-means method from the training dataset. For each scene, the intention points for the two target agents are normalized based on the focal agent’s coordinate system. The other components of the decoder are identical to those used in the Joint prediction model.

Training. In the training dataset, each scene contains several agent tracks to predict, and we consider each track sequentially as the focal agent, while the closest track to the focal agent is chosen as the interacting agent. The task is to predict six possible joint future trajectories of these two agents. To improve the prediction accuracy, we employ only imitation loss at each decoding level.

In the joint prediction model, we aim to predict the joint and scene-level future trajectories of the two agents. Therefore, we backpropagate the loss through the joint future trajectories of the two agents that most closely match the ground truth (i.e., have the least sum of displacement errors). In the marginal prediction model, we backpropagate the imitation loss to the individual agent through the posi-

tive GMM component that corresponds to the closest intention point to the endpoint of the ground-truth trajectory.

Our models are trained for 30 epochs using the AdamW optimizer with a weight decay of 0.01. The learning rate starts with 1e-4 and decays by a factor of 0.5 every 3 epochs after 15 epochs. We also clip the gradient norm of the network parameters with the max norm of the gradients as 5. We train the models using 4 NVIDIA Tesla V100 GPUs, with a batch size of 64 per GPU.

Testing. There are three types of agents in the testing dataset, which are vehicle, pedestrian, and cyclist. For the vehicle-vehicle interaction, we randomly select one of the two vehicles as the focal agent. For other types of interaction pairs (*e.g.*, cyclist-vehicle and pedestrian-vehicle), we consider the cyclist or pedestrian as the focal agent. For the marginal prediction model, we employ the Expectation-Maximization (EM) method to aggregate trajectories for each agent. Specifically, we use the EM method to obtain 6 marginal trajectories (along with their probabilities) from the 64 trajectories predicted for each agent. Then, we consider the top 6 joint predictions from the 36 possible combinations of the two agents, where the confidence of each combination is the product of the marginal probabilities.

A.2. Planning-oriented model

Model inputs. In each scene, we consider the AV and its 10 surrounding agents to perform planning for the AV and prediction for other agents. The AV’s current state is the origin of the local coordinate system. The historical states of all agents in the past two seconds are extracted; for each agent, we find its nearby 6 drivable lanes and 4 crosswalks. Additionally, we extract the AV’s traversed lane waypoints from its ground truth future trajectory and use a cubic spline to interpolate these waypoints to generate the AV’s reference route. The reference route extends 100 meters ahead of the AV and contains 1000 waypoints with 0.1 meters intervals. It is represented as a tensor with shape (1000×5) . The reference route tensor also contains information on the speed limit and stop points in addition to positions and headings.

Model structure. For each agent, its scene context tensor is created as a concatenation of all agents’ historical states and encoded local map elements, resulting in a tensor of shape (91×256) . In the decoding stage, a learnable modality embedding of size $(11 \times 6 \times 256)$ and the agent’s historical encoding are used as input to the level-0 decoder, which outputs six possible trajectories along with corresponding scores. In the level- k decoder, the future encodings of all agents are obtained through a self-attention module of size (11×256) , and are concatenated with the scene context tensor from the encoder. This concatenation generates an updated scene context tensor with a shape of (102×256) . When decoding an agent’s future trajectory

at the current level, the future encoding of that agent in the scene context tensor is masked to avoid using its future information.

Training. In data processing, we filter those scenes where the AV’s moving distance is less than 5 meters (*e.g.*, when stopping at a red light). Similarly, we perform joint future prediction and calculate the imitation loss through the joint future that is closest to the ground truth. The weights for the imitation loss and interaction loss are set to $w_1 = 1, w_2 = 0.1$. Our model is trained for 20 epochs using the AdamW optimizer with a weight decay of 0.01. The learning rate is initialized to 1e-4 and decreases by a factor of 0.5 every 2 epochs after the 10th epoch. We train the model using an NVIDIA RTX 3080 GPU, with a batch size of 32.

Testing. In open-loop testing, we check collisions between the AV’s planned trajectory and other agents’ ground-truth future trajectories, and we count a miss if the distance between AV’s planned state at the final step and the ground-truth state is larger than 4.5 meters. The planning errors and prediction errors are calculated according to the most-likely trajectories scored by the model. In closed-loop testing, the AV plans a trajectory at every timestep and executes the first step of the plan.

A.3. Baseline methods

To validate the planning capability of our model, we introduce the following imitation learning-based planning baselines.

Vanilla Imitation Learning (IL): A simplified version of our model that directly outputs the planned trajectory of the AV without explicitly reasoning other agents’ future trajectories. The plan is only a single-modal trajectory. The original encoder part of our model is utilized, but only one decoder layer with the ego agent’s historical encoding as query is used to decode the AV’s plan.

Deep Imitative Model (DIM): A probabilistic planning method that aims to generate expert-like future trajectories $q(\mathbf{S}_{1:T}|\phi) = \prod_{t=1}^T q(\mathbf{S}_t|\mathbf{S}_{1:t-1}, \phi)$ given the AV’s observations ϕ . We follow the original open-source DIM implementation and use the rasterized scene image $\mathbb{R}^{200 \times 200 \times 3}$ and the AV’s historical states $\mathbb{R}^{11 \times 5}$ as the observation. We use a CNN to encode the scene image and an RNN to encode the agent’s historical states. The AV’s future state is decoded (as a multivariate Gaussian distribution) in an autoregressive manner. In testing, DIM requires a specific goal \mathcal{G} to direct the agent to the goal, and a gradient-based planner maximizes the learned imitation prior $\log q(\mathbf{S}|\phi)$ and the test-time goal likelihood $\log p(\mathcal{G}|\mathbf{S}, \phi)$.

Robust Imitative Planning (RIP): An epistemic uncertainty-aware planning method that is developed upon DIM and shows good performance in conducting robust planning in out-of-distribution (OOD) scenarios. Specifi-

cally, we employ the original open-source implementation and choose the worst-case model that has the worst likelihood $\min_d \log q(\mathbf{S}_{1:T}|\phi)$ among $d = 6$ trained DIM models and improve it with a gradient-based planner.

Conservative Q-Learning (CQL): A widely-used offline reinforcement learning algorithm that learns to make decisions from offline datasets. We implement the CQL method with the d3rlpy offline RL library. The RL agent takes the same state inputs as the DIM method and outputs the target pose of the next step ($\Delta x, \Delta y, \Delta \theta$) relative to the agent’s current position. The reward function is the distance traveled per step plus an extra reward for reaching the goal, *i.e.*, $r_t = \Delta d_t + 10 \times \mathbb{1}(d(s_t, s_{goal}) < 1)$. Since the dataset only contains perfect driving data, no collision penalty is included.

Differentiable Integrated Prediction and Planning (DIPP): A joint prediction and planning method that uses a differentiable motion planner to optimize the trajectory according to the prediction result. We adopt the original open-source implementation and the same state input setting. We increase the historical horizon to 20 and the number of prediction modalities from 3 to 6. In open-loop testing, we utilize the results from the DIPP prediction network without trajectory planning (refinement).

MultiPath++: A high-performing motion prediction model that is based on the context-aware fusion of heterogeneous scene elements and learnable latent anchor embeddings. We utilize the open-source implementation of MultiPath++ that achieved state-of-the-art prediction accuracy on the WOMD motion prediction benchmark. We train the model to predict 6 possible trajectories and corresponding scores for the ego agent using the same dataset. In open-loop testing, only the most-likely trajectory will be used as the plan for the AV.

Motion Transformer (MTR)-e2e: A state-of-the-art prediction model that occupies the first place on the WOMD motion prediction leaderboard. We follow the original open-source implementation of the context encoder and MTR decoder. However, we modified the decoder to use an end-to-end variant of MTR that is better suited for the open-loop planning task. Specifically, only 6 learnable motion query pairs are used to decode 6 possible trajectories and scores. The same dataset is used to train MTR-e2e model, and the data is processed according to the MTR context inputs.

A.4. Refine motion planner

Inverse dynamic model. To convert the initial planned trajectory to control actions $\{a_t, \delta_t\}$ (*i.e.*, acceleration and yaw rate), we utilize the following inverse dynamic model.

$$\begin{aligned}\Phi^{-1} : v_t &= \frac{\Delta p}{\Delta t} = \frac{\| p_{t+1} - p_t \|}{\Delta t}, \\ \theta_t &= \arctan \frac{\Delta p_y}{\Delta p_x}, \\ a_t &= \frac{v_{t+1} - v_t}{\Delta t}, \\ \delta_t &= \frac{\theta_{t+1} - \theta_t}{\Delta t},\end{aligned}\tag{6}$$

where p_t is a predicted coordinate in the trajectory, and Δt is the time interval.

Dynamic model. To derive the coordinate and heading $\{p_{xt}, p_{yt}, \theta\}$ from control actions, we adopt the following differentiable dynamic model.

$$\begin{aligned}\Phi : v_{t+1} &= a_t \Delta t + v_t, \\ \theta_{t+1} &= \delta_t \Delta t + \theta_t, \\ p_{xt+1} &= v_t \cos \theta_t \Delta t + p_{xt}, \\ p_{yt+1} &= v_t \sin \theta_t \Delta t + p_{yt}.\end{aligned}\tag{7}$$

Motion Planner. We use a differentiable motion planner proposed in DIPP to plan the trajectory for the AV. The planner takes as input the initial control action sequence derived from the planned trajectory given by our model. We formulate each planning cost term c_i as a squared vector-valued residual, and the motion planner aims to solve the following nonlinear least squares (NLS) problem:

$$\mathbf{u}^* = \arg \min_{\mathbf{u}} \frac{1}{2} \sum_i \| \omega_i c_i(\mathbf{u}) \|^2,\tag{8}$$

where \mathbf{u} is the sequence of control actions, and ω_i is the weight for cost c_i .

We consider a variety of cost terms as proposed in DIPP, including travel speed, control effort (acceleration and yaw rate), ride comfort (jerk and change of yaw rate), distance to the reference line, heading difference, as well as the cost of violating traffic light. Most importantly, the safety cost takes all other agents’ predicted states into consideration and avoids collision with them, as illustrated in DIPP.

We use the Gauss-Newton (GN) method to solve the optimization problem. The maximum number of iterations is 30, and the step size is 0.2. We use the best solution obtained during the iteration process as the final plan to execute.

Learning cost function weights. Since the motion planner is differentiable, we can learn the weights of the cost terms by differentiating through the optimizer. We use the imitation learning loss below (average displacement error and final displacement error) to learn the cost weights, as well as minimize the sum of cost values. We set the maximum number of iterations to 3 and the step size to 0.5 in the

motion planner. We use the Adam optimizer with a learning rate of 1e-4 to train the cost function weights; the batch size is 32 and the total number of training steps is 10,000.

$$\mathcal{L} = \lambda_1 \sum_t \|\hat{s}_t - s_t\|^2 + \lambda_2 \|\hat{s}_T - s_T\|^2 + \lambda_3 \sum_i \|c_i\|^2, \quad (9)$$

where $\lambda_1 = 1$, $\lambda_2 = 0.5$, $\lambda_3 = 0.001$ are the loss function weights.

B. Additional Quantitative Results

B.1. Interaction Prediction

Table 6 displays the per-category performance of our models on the WOMD interaction prediction benchmark, in comparison with the MTR model. The GameFormer joint prediction model exhibits the lowest minFDE in all object categories, indicating the advantage of our model and joint training of interaction patterns. Our GameFormer model surpasses MTR in the cyclist category and achieves comparable performance with MTR in other categories, albeit with a much simpler structure than MTR.

Table 6. Per-class performance of interaction prediction on the WOMD interaction prediction benchmark

Class	Model	minADE (↓)	minFDE (↓)	Miss rate (↓)	mAP (↑)
Vehicle	MTR	0.9793	2.2157	0.3833	0.2977
	GF (J)	0.9822	2.0745	0.3785	0.1856
	GF (M)	1.0499	2.4044	0.4321	0.2469
Pedestrian	MTR	0.7098	1.5835	0.3973	0.2033
	GF (J)	0.7279	1.4894	0.4272	0.1505
	GF (M)	0.7978	1.8195	0.4713	0.1962
Cyclist	MTR	1.0652	2.3908	0.5428	0.1102
	GF (J)	1.0383	2.2480	0.5536	0.0768
	GF (M)	1.0686	2.4199	0.5765	0.1338

B.2. Abalation study

Influence of loss function on intermediate layers. Our model generates intermediate outputs as trajectories, allowing us to compute the loss on the output of all layers instead of just the final layer, as is standard. We investigate the impact of applying imitation learning loss solely to the final layer compared to all layers on the performance of our model in open-loop planning. This approach reduces the decoder part of our model to a multi-layer Transformer that does not produce intermediate states. The results presented in Table 7 demonstrate that applying the loss only to the final output can significantly degrade the performance of the model, highlighting the importance of regularizing the output of intermediate states.

Table 7. Influence of the loss function on open-loop planning

	Planning ADE	Collision Rate	Miss Rate	Prediction ADE
All layers (Base)	0.8329	0.0198	0.0753	0.8547
Final layer	0.9584	0.0353	0.0988	0.9637

Effects of decoding levels on closed-loop planning.

We investigate the influence of decoding levels on closed-loop planning performance, using the success rate (without collision) as the main metric. Additionally, we report the inference time of the prediction network (without the refine motion planner) in closed-loop planning, which is executed on an NVIDIA RTX 3080 GPU. The results in Table 8 reveal that increasing the decoding layers could lead to a higher success rate, and adding one layer of interaction modeling can bring significant improvement compared to level-0. In closed-loop testing, the success rate plateaus when the decoding level reaches 2, but the computation time continues to increase. Therefore, using two reasoning levels in our model may achieve a good balance between performance and efficiency in practical applications.

Table 8. Effects of decoding levels on closed-loop planning

Level	Closed-loop testing	
	Success rate (%)	Inference (ms)
0	89.5	31.8
1	92.25	44.1
2	94	56.7
3	94.5	66.5
4	94.5	79.2

C. Additional Qualitative Results

C.1. Interaction Prediction

Fig. 6 presents additional qualitative results of our GameFormer framework in the interaction prediction task, showcasing the ability of our method to handle a variety of interaction pairs and urban driving scenarios.

C.2. Level- k Prediction

Fig. 7 illustrates the most-likely joint trajectories of the target agents at different interaction levels. The results demonstrate that our proposed framework is capable of refining the prediction results in the iterated interaction process. At level-0, the target agents are predicted rather independently, and their trajectories may collide. However, through iterative refinement, our model can output reasonable and close-to-human trajectories at the final level.

C.3. Open-loop planning

Fig. 8 provides additional qualitative results of our framework in the open-loop planning task, which depict the ability of our model to plan the trajectory of the AV and predict its neighboring agents.

C.4. Closed-loop planning

We visualize the closed-loop planning performance of our method through videos available on the project website, including several highly interactive scenarios.

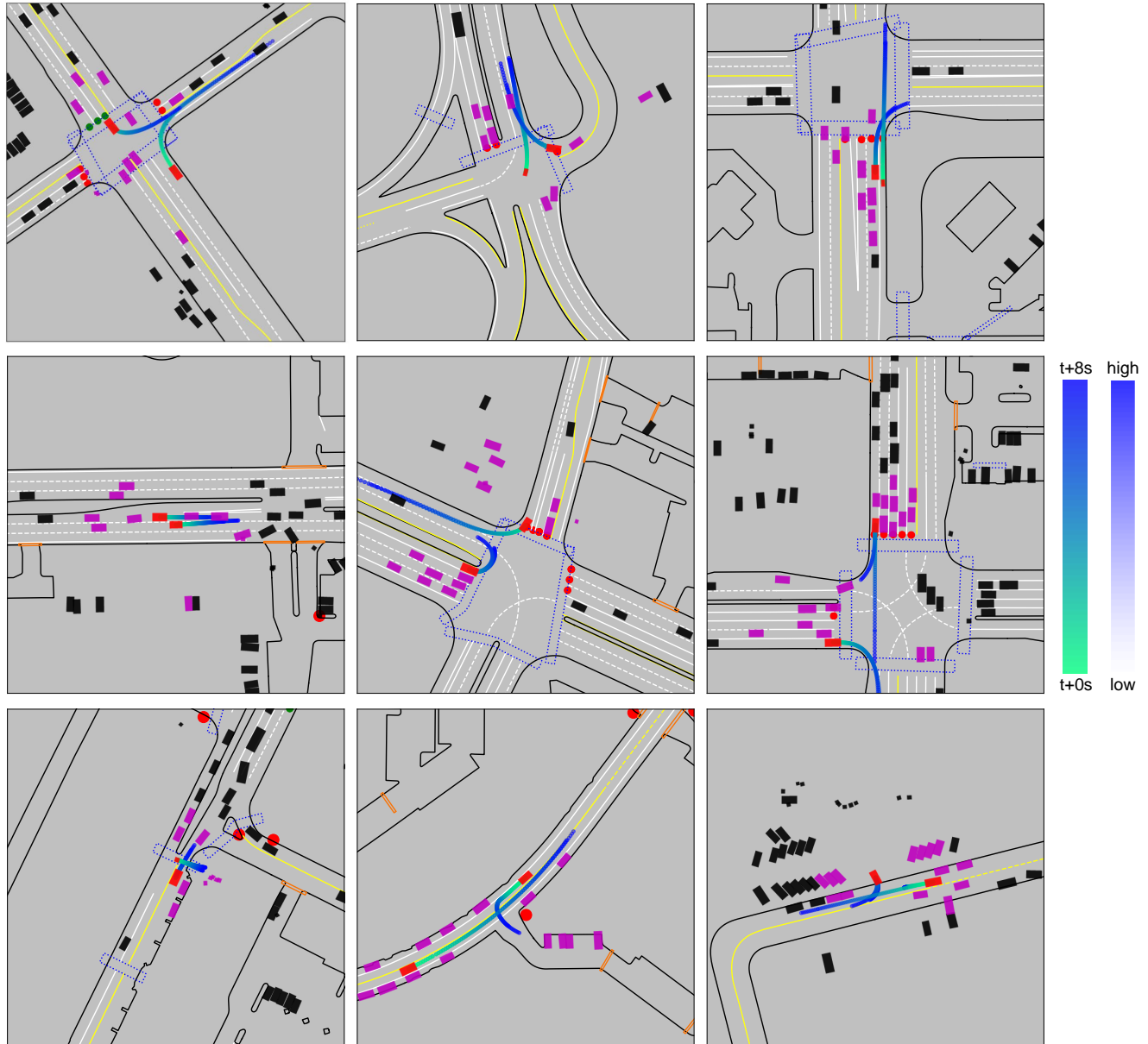


Figure 6. Additional qualitative results of interaction prediction. The red boxes are interacting agents to predict, and the magenta boxes are background neighboring agents. Six joint trajectories of the two interacting agents are predicted.

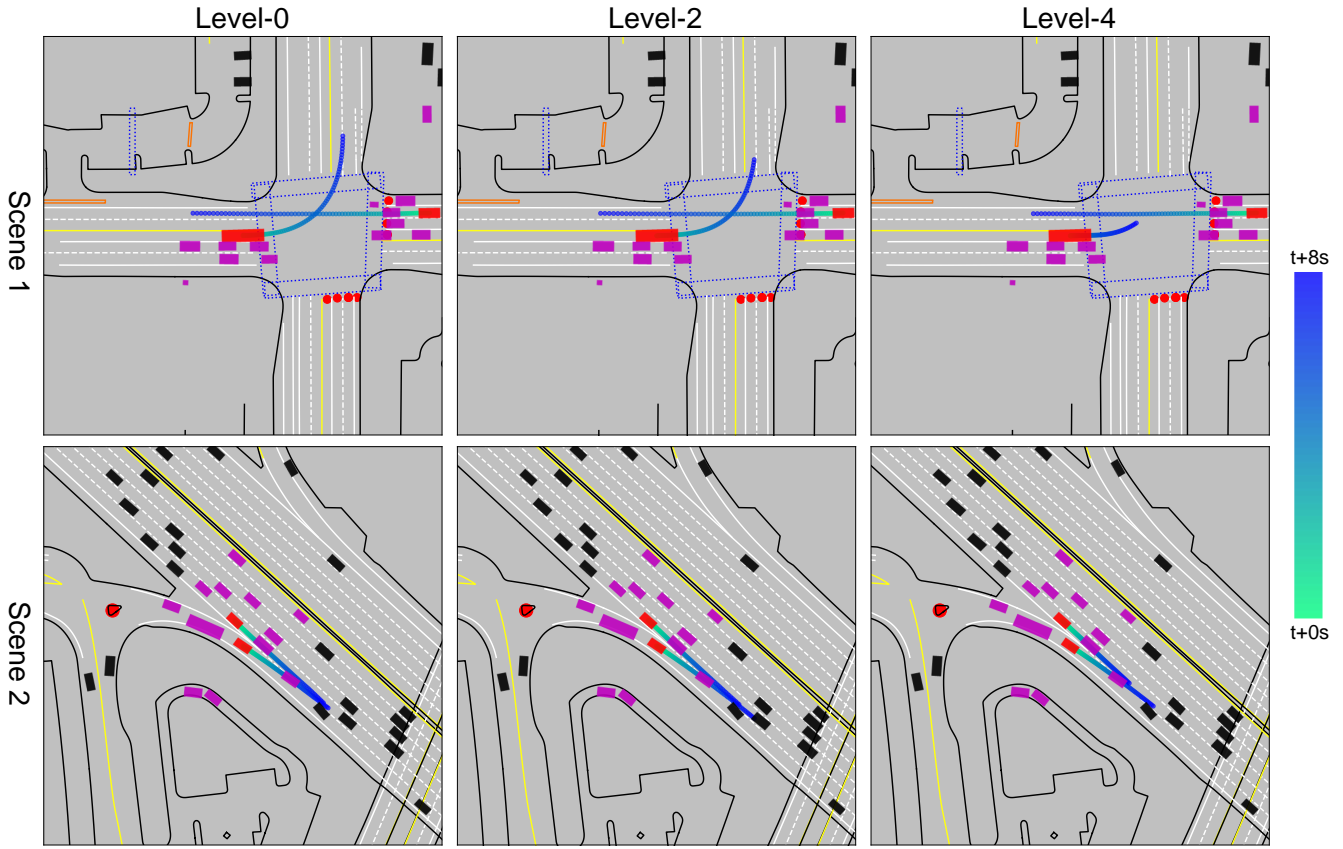


Figure 7. Prediction results of the two interacting agents at different reasoning levels. Only the most-likely joint trajectories of the target agents are displayed for clarity.

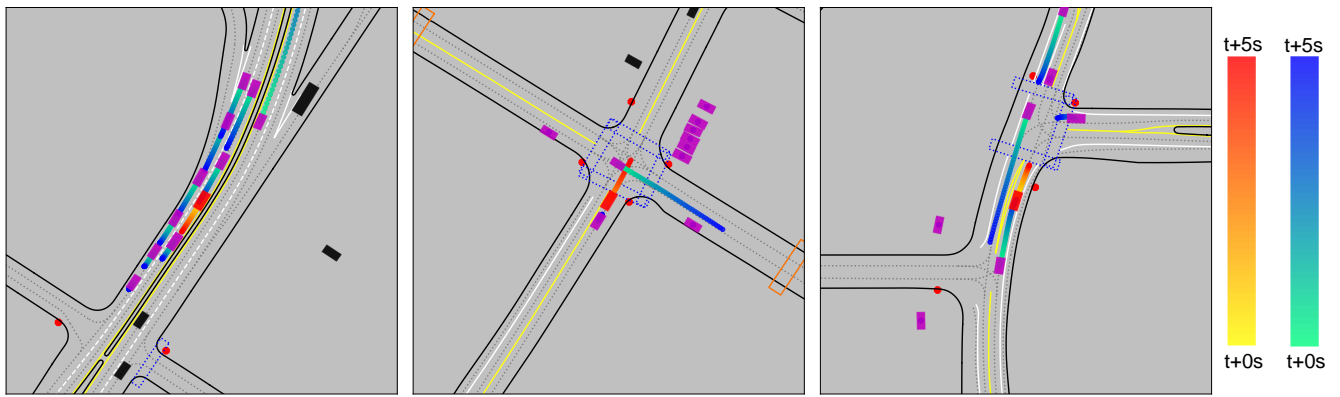


Figure 8. Additional qualitative results of open-loop planning. The red box is the AV and the magenta boxes are its neighboring agents; the red trajectory is the plan of the AV and the blue ones are the predictions of neighboring agents